HHS Public Access

Author manuscript

Neuroimage. Author manuscript; available in PMC 2015 June 03.

Published in final edited form as:

Neuroimage. 2006 May 15; 31(1): 301–307. doi:10.1016/j.neuroimage.2005.12.024.

Network modulation by the subthalamic nucleus in the treatment of Parkinson's disease

Maja Trošt[a,b], **Sherwin Su**[a], **Philip Su**[c], **Ruoh-Fang Yen**[c], **Ham-Min Tseng**[c], **Anna Barnes**[a], **Yilong Ma**[a,d], and **David Eidelberg**[a,d,*]

[a]Center for Neurosciences, Institute for Medical Research, North Shore-Long Island Jewish Health System, Manhasset, NY 11030, USA

[b]Department of Neurology, University Medical Centre, Ljubljana, Slovenia

[c]Departments of Neurology, Neurosurgery, and Nuclear Medicine, National Taiwan University Hospital, Taipei, Taiwan

[d]Departments of Neurology and Medicine, New York University School of Medicine, New York, NY 10016, USA

Abstract

Deep brain stimulation of the subthalamic nucleus (STN DBS) has become an accepted tool for the treatment of Parkinson's disease (PD). Although the precise mechanism of action of this intervention is unknown, its effectiveness has been attributed to the modulation of pathological network activity. We examined this notion using positron emission tomography (PET) to quantify stimulation-induced changes in the expression of a PD-related covariance pattern (PDRP) of regional metabolism. These metabolic changes were also compared with those observed in a similar cohort of patients undergoing STN lesioning.

We found that PDRP activity declined significantly ($P < 0.02$) with STN stimulation. The degree of network modulation with DBS did not differ from that measured following lesioning ($P = 0.58$). Statistical parametric mapping (SPM) revealed that metabolic reductions in the internal globus pallidus (GPi) and caudal midbrain were common to both STN interventions ($P < 0.01$), although declines in GPi were more pronounced with lesion. By contrast, elevations in posterior parietal metabolism were common to the two procedures, albeit more pronounced with stimulation.

These findings indicate that suppression of abnormal network activity is a feature of both STN stimulation and lesioning. Nonetheless, these two interventions may differ metabolically at a regional level.

Introduction

The subthalamic nucleus (STN) plays a critical role in the modulation of cortico-striato-pallido-thalamocortical (CSPTC) motor pathways (Wichmann and DeLong, 1996; Hamani

*Corresponding author. Center for Neurosciences, Institute for Medical Research, North Shore-Long Island Jewish Health System, 350 Community Drive, Manhasset, NY 11030, USA. Fax: +1 516 562 1008. david1@nshs.edu (D. Eidelberg).

et al., 2004). The motor symptoms of Parkinson's disease (PD) are associated with increased STN activity, which results in excessive inhibitory outflow from the basal ganglia to the thalamus and brainstem (Vitek and Giroux, 2000). A variety of stereotaxic surgical approaches have been introduced to modulate STN neural activity and restore normal functioning to motor CSPTC circuitry (Lozano and Mahant, 2004).

Positron emission tomography (PET) can provide useful information concerning the functional status of CSPTC pathways in PD (Eidelberg et al., 2000). In particular, network analyses of regional PET data have consistently revealed the presence of a reproducible abnormal spatial covariance pattern associated with parkinsonism (Eidelberg et al., 1994; Moeller et al., 1999; Lozza et al., 2004; Asanuma et al., 2005a). This PD-related pattern (PDRP) is characterized by pallido-thalamic and pontine hypermetabolism associated with relative metabolic decrements in premotor, prefrontal, and posterior parietal cortical regions (Carbon and Eidelberg, 2002; Asanuma et al., 2005a). We have attributed this abnormal metabolic topography to overactivity of internal pallidal (GPi) afferents from STN and consequent increases in inhibitory pallidal outflow to the ventral thalamus and pons (Eidelberg et al., 1994, 1997). To test this hypothesis, we quantified PDRP expression in patients with advanced disease undergoing stereotaxic subthalamotomy (Su et al., 2001). Indeed, STN lesioning was found to produce a marked and sustained reduction in network activity in human subjects (Trošt et al., 2003).

The activity of STN and its projection pathways can also be modulated by deep brain stimulation (DBS) (Vitek and Giroux, 2000; Benabid, 2003; Lozano and Mahant, 2004). The precise mechanism by which STN DBS achieves therapeutic benefit is not known. Several experimental studies have pointed to local inhibition as the predominant effect of this intervention in PD (Filali et al., 2004; Lozano and Mahant, 2004). Despite the controversy surrounding the local effects of stimulation (McIntyre et al., 2004a,b), the modulation of pathological network activity is likely to be the basis for clinical benefit in STN DBS as well as in other basal ganglia interventions for PD, including lesioning of critical nodes of the CSPTC motor loop (Eidelberg et al., 1996; Fukuda et al., 2001; Su et al., 2001; Carbon and Eidelberg, 2002; Eckert and Eidelberg, 2005).

In the current study, we examined the notion that STN lesioning and stimulation were mechanistically similar at a system level. We used PET to compare the metabolic effects of the two stereotaxic interventions in patients with advanced PD who were offered one or the other treatment. Specifically, network analysis was employed to determine whether PDRP suppression is a feature of STN stimulation as well as lesioning, and whether the degree of network modulation differed with these treatment approaches.

Materials and methods

Subjects

We studied six patients with advanced stage (Hoehn and Yahr Stage IV) PD who underwent STN DBS implantation at the National Taiwan University Hospital in Taipei, Taiwan. Electrode placement was unilateral in four patients and bilateral in two. Medtronic 3389 DBS leads were implanted into the STN following microelectrode mapping according to

methods reported by us previously with subthalamotomy (Su et al., 2002). Postoperative MRI was done within 1 week to verify the location of the electrode. Stimulation settings were adjusted to achieve maximal improvement in contralateral limb rigidity and akinesia as each of the four electrode contacts was activated. Patient characteristics and stimulation parameters are presented in Table 1.

These participants were demographically similar to a cohort of six advanced PD patients reported from the same center, who were treated with unilateral subthalamotomy (Su et al., 2001, 2002; Trošt et al., 2003). Subject age, symptom duration, and composite motor ratings (UPDRS part III, items 18–31) at the time of surgery did not differ significantly for the two treatment groups [age (mean±SE): 60.0±3.1 and 56.2±3.7 years ($P = 0.50$); symptom duration: 10.3±1.2 and 10.5±1.4 years ($P = 0.93$); motor ratings: 52.2±4.9 and 64.4±8.7 ($P = 0.23$) for the STN stimulation and lesion groups, respectively]. Assignment to treatment group was determined by the patient's choice after a full explanation of the risks and benefits of the two procedures, as well as his/her access to specialized neurological services. Written informed consent was obtained from all participants.

Positron emission tomography

Patients were scanned approximately 6 months following STN DBS implantation. While in a fasting state, each patient underwent FDG PET imaging as described previously using the GE Advance tomograph (General Electric Medical Systems, Milwaukee, WI) at National Taiwan University Hospital in Taipei, Taiwan (Su et al., 2001; Trošt et al., 2003). Scanning in 3D mode was performed in the ON and OFF DBS conditions, defined by the presence or absence of stimulation for at least 24 h prior to the imaging sessions. The two test conditions were performed on separate days with the order randomized across subjects. All scans were conducted following a 12-h medication washout. Subjects were rated according to UPDRS at each scanning session.

Data analysis

Data processing was performed using SPM99 (Wellcome Department of Cognitive Neurology, London, UK) as described in detail previously (Fukuda et al., 2001; Trošt et al., 2003). Images from patients who had STN DBS placed in the left hemisphere were reversed such that all stimulated hemispheres appeared on the right. All images were then transformed into Montreal Neurological Institute (MNI) space (Collins et al., 1994) and smoothed using 10-mm FWHM Gaussian smoothing kernel prior to statistical analysis. Global intensity was normalized by scaling each voxel in each image to its own mean global counts.

Local changes in glucose utilization with STN stimulation

To identify changes in regional metabolism associated with STN stimulation, we used the paired t test option in SPM99 comparing ON and OFF scans across the eight stimulated hemispheres. We also used SPM tools to compare stimulation-induced metabolic changes with those occurring following STN lesion. Firstly, we searched for regions where the metabolic changes with STN stimulation and lesion were in opposing directions (i.e., increasing in one and decreasing in the other or vice versa). Secondly, we employed

conjunction analysis (Price and Friston, 1997) to identify regions where the two interventions gave rise to similar changes (i.e., increases or decreases) in local glucose utilization. Preoperative UPDRS motor scores were entered into the SPM model as nuisance variables to account for potential group difference in disease severity at baseline. Treatment-related metabolic effects in these areas were quantified as the percent change with respect to baseline in 5 mm^3 volumes centered on the peak voxel within each cluster (Su et al., 2001; Trošt et al., 2003).

All SPM analyses were performed within the hypothesis-testing mask described by us previously (Fukuda et al., 2001). This space was comprised of voxel clusters known to be metabolically abnormal in PD ($P < 0.001$). The mask included the basal ganglia, thalamus, pons, and cerebellum, as well as the premotor, prefrontal, anterior cingulate, and posterior parietal cortical regions. Metabolic changes within this mask were considered significant for $P < 0.01$, uncorrected for multiple regional comparisons. For exploratory purposes, we also reported regional changes in the mask at the $P < 0.05$ level (uncorrected) if they coincided with key elements of the PDRP spatial covariance topography. Metabolic changes outside the mask were considered to be hypothesis generating and significant for $P < 0.05$, corrected.

Network modulation by STN stimulation

We also assessed changes in the expression of the PDRP (Fig. 1A) during stimulation. This was accomplished by prospectively quantifying individual subject scores for this pattern in the ON and OFF states (Fukuda et al., 2001; Su et al., 2001). Fully automated voxel-based network computations (software available at http://neuroscience-nslij.org/Methods/software.html) were performed on a hemisphere-by-hemisphere basis as described previously (Fukuda et al., 2001; Trošt et al., 2003). To compare network changes with stimulation to those following lesioning, we included scans from patients imaged before and 3 months following unilateral subthalamotomy (Su et al., 2001). All PDRP computations were performed blind to subject, surgical procedure (DBS/lesion), hemisphere (operated/non-operated), treatment condition (ON/OFF, POST/PRE), and clinical status (UPDRS motor ratings). Network activity changes with intervention (ON–OFF or POST–PRE) were computed for each subject and hemisphere. PDRP changes with stimulation and lesioning were compared to one another as well as to control values (i.e., those from the non-operated contralateral hemispheres) using ANOVA with post hoc comparisons, adjusting for group differences in baseline UPDRS motor ratings. All statistical comparisons of PDRP activity within and between groups were considered significant for $P < 0.05$.

Results

Metabolic changes with STN stimulation

STN stimulation resulted in significant improvement in contralateral limb UPDRS motor ratings (−46.5%, $P < 0.001$). SPM analysis of ON and OFF scans disclosed several areas of metabolic change in the stimulated hemispheres (Table 2). STN stimulation reduced glucose utilization (ON < OFF) in a cluster of voxels within the rostral pons and midbrain. Additionally, stimulation was associated with ipsilateral decrements in the primary motor

cortex (BA 4), supplementary motor area (SMA; BA 6), and in the cerebellar vermis. Increases with stimulation (ON > OFF) were observed ipsilaterally in the parietal lobe (BA 7) and to a lesser degree in prefrontal cortex (BA 9). We also found that UPDRS motor scores correlated ($r > 0.83$, $P < 0.001$) with regional metabolic values in the midbrain, cerebellum, and motor cortex. Stimulation-induced changes in regional metabolism were not detected in the non-operated hemisphere or outside the hypothesis-testing mask.

Next we quantified the expression of the PDRP network (Fig. 1A) in the ON and OFF conditions. We found that STN stimulation resulted in a mean decline in PDRP activity ($P < 0.02$, Fig. 1B), with reductions in 7/8 treated hemispheres. The magnitude of PDRP reduction was greater in the hemispheres of patients undergoing bilateral stimulation relative to their unilaterally stimulated counterparts ($P < 0.01$). In addition, individual PDRP scores correlated ($r = 0.63$, $P < 0.01$) with contralateral limb UPDRS motor scores. Changes in both local metabolism and PDRP expression were not significant ($P > 0.5$) in the non-operated hemispheres.

Comparison of STN stimulation and lesioning

SPM conjunction analysis revealed that STN stimulation and lesioning shared several local metabolic features. These results are summarized in Table 3. Metabolic declines in the midbrain, GPi, and in the cingulate motor region (BA 24/6) were common to both interventions (Fig. 2, top). Metabolic increases in the parietal cortex (BA 7/39/40) were also common to the two surgical procedures (Fig. 3, left). Notably, treatment-related metabolic declines in the pallidum were relatively more pronounced following STN lesion ($P < 0.01$) (Fig. 2, bottom), while metabolic increases in the parietal cortex were comparatively greater with stimulation ($P < 0.05$) (Fig. 3, right). We did not identify any significant regions in which the two interventions gave rise to metabolic changes of opposite direction.

Network analysis revealed that the magnitude of PDRP suppression was similar for both STN stimulation and lesioning ($P = 0.58$), although both differed significantly ($P < 0.05$) from control values (Fig. 1B).

Discussion

Metabolic changes with STN stimulation

In advanced PD, significant clinical benefit can be achieved with either stereotaxic lesioning or high-frequency stimulation of the STN (Lozano and Mahant, 2004; Okun and Vitek, 2004). Although the therapeutic outcome is similar for both these interventions, the mechanisms underlying STN lesioning and stimulation may be different (McIntyre et al., 2004a,b). Indeed, evidence from experimental animal models has suggested that neurochemical and physiologic changes with stimulation at the target site may not be explained simply by inhibition (Windels et al., 2000; Hashimoto et al., 2003). Nonetheless, neural recordings during DBS in awake patients have indicated that local inhibition is an important feature of therapeutic DBS (Dostrovsky and Lozano, 2002).

Our PET findings of altered glucose utilization during STN stimulation are generally compatible with prior studies of stimulation effects on brain metabolism in PD. These

investigations revealed local metabolic changes at or near the surgical target and at remote nodes within CSPTC loops and related pathways (Fukuda et al., 2001, 2004; Strafella et al., 2003; Hilker et al., 2004; Vafaee et al., 2004). In the current study, we found that the effects of STN DBS on regional metabolism were generally similar to those identified following subthalamotomy (Su et al., 2001; Trošt et al., 2003). Specifically, declines in glucose utilization during STN stimulation were detected in the rostral pons and midbrain in proximity to the upper portion of the pedunculopontine nucleus (PPN, Pahapill and Lozano, 2000). Metabolic reductions in these regions have also been reported following STN lesioning (Su et al., 2001; Trošt et al., 2003), suggesting diminished outflow from the STN target nucleus to the brainstem in both interventions.

Comparison of scans ON and OFF stimulation also revealed metabolic decreases with stimulation in the precentral gyrus (BA 4) and caudal SMA (BA 6) and in the cerebellar vermis. Discrete metabolic reductions in motor cortical and cerebellar areas distant from the stimulation site have been reported with STN DBS (Hershey et al., 2003; Hilker et al., 2004; Payoux et al., 2004). Our data are compatible with the notion of CSPTC hyperactivity in resting PD patients, which may be reduced by stimulation. The suppression of PD tremor by STN DBS may also explain the functional changes detected in these regions (Fukuda et al., 2004; Trošt et al., 2004).

The current study further revealed stimulation-mediated metabolic increases in the posterior parietal lobe (BA 7). This finding is compatible with prior studies showing similar parietal changes with STN stimulation (Hilker et al., 2004; Vafaee et al., 2004). The specific cause for this localized increase is not known, although such remote cortical changes are not likely to occur in isolation. Indeed, we found that stimulation also increased glucose utilization in the prefrontal cortex (BA 9), albeit of lesser magnitude than in the parietal lobe (see Table 2). These findings may be attributed to potentiation of prefrontal–parietal pathways, as observed both in the resting state (Sestini et al., 2002; Hilker et al., 2004) and during motor learning (Carbon et al., 2003). Increases in the activity of this transcortical projection system with stimulation may be responsible for the improvement in working memory and other forms of executive functioning reported in PD patients undergoing DBS (Jahanshahi et al., 2000; Pillon et al., 2000; Fukuda et al., 2002).

Our results generally accord with prior PET studies of STN stimulation. Moreover, in many of the regions found to be modulated by DBS, local metabolism correlated significantly with UPDRS motor ratings. This suggests a direct association between clinical outcome and stimulation-mediated metabolic changes in the brainstem, cerebellum, and motor cortex. Nonetheless, we found several inconsistencies with respect to earlier studies, which might be referable to methodological differences such as whether the local changes with stimulation were detected by imaging regional cerebral blood flow as opposed to metabolism. Indeed, an uncoupling of these two parameters during treatment has recently been suggested (Vafaee et al., 2004; Asanuma et al., 2005b).

The local metabolic changes seen with SPM analysis are compatible with downward modulation of disease-related network activity. Using an automated voxel-driven network quantification approach, we found that STN stimulation was associated with a decline in

PDRP expression, as seen in other antiparkinsonian interventions (Carbon and Eidelberg, 2002; Eckert and Eidelberg, 2005). Likewise, with STN DBS, individual differences in PDRP expression correlated with UPDRS motor ratings, as previously observed with other stereotaxic surgical approaches (Fukuda et al., 2001; Trošt et al., 2003) and with levodopa (Feigin et al., 2001). Additionally, we found that network suppression was significantly greater for hemispheres undergoing ipsilateral as well as contralateral stimulation. Thus, STN DBS can potentiate network modulation bilaterally, as described in PD patients undergoing unilateral GPi stimulation (Fukuda et al., 2001). The mechanism of this bilateral effect is unknown, although transhemisphere interactions at thalamic or cortical levels may be involved (Parent and Hazrati, 1995; Eidelberg et al., 1996). Augmentation of network modulation by contralateral stimulation supports the utility of bilateral DBS interventions, even in asymmetrical parkinsonism (Kumar et al., 1999).

Comparison of STN stimulation and lesioning

Although of limited size, our STN DBS cohort allowed for direct metabolic comparison with similar PD patients undergoing subthalamotomy. We found that the regional changes in glucose utilization occurring with STN stimulation parallel those following stereotaxic ablation of the same structure. Specifically, conjunction analysis disclosed that declines in pallidal and brainstem metabolic activity occurred with both interventions. This analysis also detected metabolic decrements in the vicinity of the anterior cingulate region, as well as shared metabolic increases in parietal association areas. In an exploratory analysis, we used other SPM tools to search for regions where metabolic changes with the two STN interventions were in opposite directions. However, we could not identify such regions even at a very liberal threshold. In keeping with these observations, prospective network quantification disclosed similar levels of PDRP suppression with the two procedures. Overall, these findings support the notion that STN DBS and lesioning for the treatment of PD provide benefit through similar functional mechanisms (Filali et al., 2004; Lozano and Mahant, 2004).

Nonetheless, from a metabolic standpoint, these two procedures are by no means identical. Although both STN lesioning and stimulation lower glucose utilization in GPi, this effect is more pronounced with the former intervention. Local rates of glucose utilization are determined mainly by afferent synaptic activity (Auker et al., 1983; Eidelberg et al., 1997). Thus, it is likely that pallidal inputs from STN are disrupted more by lesioning than by stimulation. Activation of subthalamic projections to the pallidum has been recently observed with STN DBS in a primate model (Hashimoto et al., 2003). This may also contribute to the smaller magnitude of the metabolic reductions in GPi observed with stimulation.

We also found that metabolic increments in the posterior parietal lobe subsequent to stimulation tended to be larger than with lesioning. As mentioned above, STN DBS has been shown to enhance energy consumption in cortical association regions (Hilker et al., 2004; Vafaee et al., 2004). This finding is consistent with STN inhibition and consequent reduction in inhibitory output from GPi and substantia nigra pars reticularis (SNr). However, comparison of these stimulation-induced cortical effects to those occurring with STN lesion

is not straightforward, given the difference in sample size between the two treatment groups. Direct stimulation of STN projections to prefrontal association regions (Maurice et al., 1998) and concomitant increases in transcortical output to the parietal lobe may also contribute to the relatively greater metabolic increases noted in this region with DBS.

In summary, our findings suggest that treatment-related modulation of pathological network activity is a feature of both STN DBS and lesioning (Montgomery and Baker, 2000). While both interventions have similar effects on brain function at a network level, this does not necessarily imply commonality of mechanism at the target site (McIntyre et al., 2004a,b). Indeed, activation of STN outflow pathways by DBS may contribute to the subtle differences from lesioning noted in the globus pallidus and cerebral cortex. Further PET studies in larger cohorts will be needed to identify specific intervention-related patterns correlating with therapeutic outcome in stimulation and with lesioning (e.g., Eidelberg et al., 1996). The delineation of specific metabolic topographies associated with individual treatment approaches may prove useful in understanding the mechanisms that underlie new therapies for parkinsonism and other movement disorders.

Acknowledgments

This work was supported by NIH RO1 NS 35069. Dr. Trošt was supported by the Veola T. Kerr Fellowship of the Parkinson Disease Foundation. Dr. Eidelberg was supported by NIH K24 NS 02101. The authors wish to thank Ms. Christine Edwards and Ms. Toni Flanagan for the valuable editorial assistance.

References

Asanuma K, Ma Y, Huang C, et al. The metabolic pathology of dopa-responsive dystonia. Ann Neurol. 2005a; 57:596–600. [PubMed: 15786454]

Asanuma K, Ma Y, Huang C, Feigin A, Dhawan V, Eidelberg D. Hemodynamic and metabolic responses induced by subthalamic nucleus stimulation: An H20 and FDG PET study. NeuroImage. 2005; 26(Suppl. 1):S24.

Auker CR, Meszler RM, Carpenter DO. Apparent discrepancy between single-unit activity and [14C]deoxyglucose labeling in optic tectum of the rattlesnake. J Neurophysiol. 1983; 49:1504–1516. [PubMed: 6875635]

Benabid AL. Deep brain stimulation for Parkinson's disease. Curr Opin Neurobiol. 2003; 13:696–706. [PubMed: 14662371]

Carbon M, Eidelberg D. Modulation of regional brain function by deep brain stimulation: studies with positron emission tomography. Curr Opin Neurol. 2002; 15:451–455. [PubMed: 12151842]

Carbon M, Ghilardi MF, Feigin A, et al. Learning networks in health and Parkinson's disease: reproducibility and treatment effects. Hum Brain Mapp. 2003; 19:197–211. [PubMed: 12811735]

Collins DL, Neelin P, Peters TM, Evans AC. Automatic 3D intersubject registration of MR volumetric data in standardized Talairach space. J Comput Assist Tomogr. 1994; 18:192–205. [PubMed: 8126267]

Dostrovsky JO, Lozano AM. Mechanisms of deep brain stimulation. Mov Disord. 2002; 17(Suppl. 3):S63–S68. [PubMed: 11948756]

Eckert T, Eidelberg D. Neuroimaging and therapeutics in movement disorders. NeuroRx. 2005; 2:361–371. [PubMed: 15897956]

Efron, B.; Tibshirani, R. An Introduction to the Bootstrap. CRC Press; LLC, New York: 1994.

Eidelberg D, Moeller JR, Dhawan V, et al. The metabolic topography of parkinsonism. J Cereb Blood Flow Metab. 1994; 14:783–801. [PubMed: 8063874]

Eidelberg D, Moeller JR, Ishikawa T, et al. Regional metabolic correlates of surgical outcome following unilateral pallidotomy for Parkinson's disease. Ann Neurol. 1996; 39:450–459. [PubMed: 8619523]

Eidelberg D, Moeller JR, Kazumata K, et al. Metabolic correlates of pallidal neuronal activity in Parkinson's disease. Brain. 1997; 120(Pt. 8):1315–1324. [PubMed: 9278625]

Eidelberg, D.; Edwards, C.; Mentis, M.; Dhawan, V.; Moeller, JR. Movement Disorders: Parkinson's Disease. In: Mazziotta, JC.; Toga, AW.; Frackowiak, RSJ., editors. Brain Mapping: The Disorders. Academic Press; San Diego: 2000. p. 241-261.

Feigin A, Fukuda M, Dhawan V. Metabolic correlates of levodopa response in Parkinson's disease. Neurology. 2001; 57:2083–2088. [PubMed: 11739830]

Filali M, Hutchison WD, Palter VN, Lozano AM, Dostrovsky JO. Stimulation-induced inhibition of neuronal firing in human subthalamic nucleus. Exp Brain Res. 2004; 156:274–281. [PubMed: 14745464]

Fukuda M, Mentis MJ, Ma Y, et al. Networks mediating the clinical effects of pallidal brain stimulation for Parkinson's disease: a PET study of resting-state glucose metabolism. Brain. 2001; 124:1601–1609. [PubMed: 11459751]

Fukuda M, Ghilardi MF, Carbon M, et al. Pallidal stimulation for parkinsonism: improved brain activation during sequence learning. Ann Neurol. 2002; 52:144–152. [PubMed: 12210783]

Fukuda M, Barnes A, Simon ES, et al. Thalamic stimulation for parkinsonian tremor: correlation between regional cerebral blood flow and physiological tremor characteristics. NeuroImage. 2004; 21:608–615. [PubMed: 14980563]

Hamani C, Saint-Cyr JA, Fraser J, Kaplitt M, Lozano AM. The subthalamic nucleus in the context of movement disorders. Brain. 2004; 127:4–20. [PubMed: 14607789]

Hashimoto T, Elder CM, Okun MS, Patrick SK, Vitek JL. Stimulation of the subthalamic nucleus changes the firing pattern of pallidal neurons. J Neurosci. 2003; 23:1916–1923. [PubMed: 12629196]

Hershey T, Revilla FJ, Wernle AR, et al. Cortical and subcortical blood flow effects of subthalamic nucleus stimulation in PD. Neurology. 2003; 61:816–821. [PubMed: 14504327]

Hilker R, Voges J, Weisenbach S, et al. Subthalamic nucleus stimulation restores glucose metabolism in associative and limbic cortices and in cerebellum: evidence from a FDG-PET study in advanced Parkinson's disease. J Cereb Blood Flow Metab. 2004; 24:7–16. [PubMed: 14688612]

Jahanshahi M, Ardouin CM, Brown RG, et al. The impact of deep brain stimulation on executive function in Parkinson's disease. Brain. 2000; 123(Pt. 6):1142–1154. [PubMed: 10825353]

Kumar R, Lozano AM, Sime E, Halket E, Lang AE. Comparative effects of unilateral and bilateral subthalamic nucleus deep brain stimulation. Neurology. 1999; 53:561–566. [PubMed: 10449121]

Lozano AM, Mahant N. Deep brain stimulation surgery for Parkinson's disease: mechanisms and consequences. Parkinsonism Relat Disord. 2004; 10(Suppl. 1):S49–S57. [PubMed: 15109587]

Lozza C, Baron JC, Eidelberg D, Mentis MJ, Carbon M, Marie RM. Executive processes in Parkinson's disease: FDG-PET and network analysis. Hum Brain Mapp. 2004; 22:236–245. [PubMed: 15195290]

Maurice N, Deniau JM, Glowinski J, Thierry AM. Relationships between the prefrontal cortex and the basal ganglia in the rat: physiology of the corticosubthalamic circuits. J Neurosci. 1998; 18:9539–9546. [PubMed: 9801390]

McIntyre CC, Savasta M, Kerkerian-Le Goff L, Vitek JL. Uncovering the mechanism(s) of action of deep brain stimulation: activation, inhibition, or both. Clin Neurophysiol. 2004; 115:1239–1248. [PubMed: 15134690]

McIntyre CC, Savasta M, Walter BL, Vitek JL. How does deep brain stimulation work? Present understanding and future questions. J Clin Neurophysiol. 2004; 21:40–50. [PubMed: 15097293]

Moeller JR, Nakamura T, Mentis MJ, et al. Reproducibility of regional metabolic covariance patterns: comparison of four populations. J Nucl Med. 1999; 40:1264–1269. [PubMed: 10450676]

Montgomery EB Jr, Baker KB. Mechanisms of deep brain stimulation and future technical developments. Neurol Res. 2000; 22:259–266. [PubMed: 10769818]

Okun MS, Vitek JL. Lesion therapy for Parkinson's disease and other movement disorders: update and controversies. Mov Disord. 2004; 19:375–389. [PubMed: 15077235]

Pahapill PA, Lozano AM. The pedunculopontine nucleus and Parkinson's disease. Brain. 2000; 123(Pt. 9):1767–1783. [PubMed: 10960043]

Parent A, Hazrati LN. Functional anatomy of the basal ganglia: I. The cortico-basal ganglia-thalamocortical loop. Brain Res Brain Res Rev. 1995; 20:91–127. [PubMed: 7711769]

Payoux P, Remy P, Damier P, et al. Subthalamic nucleus stimulation reduces abnormal motor cortical overactivity in Parkinson disease. Arch Neurol. 2004; 61:1307–1313. [PubMed: 15313852]

Pillon B, Ardouin C, Damier P, et al. Neuropsychological changes between "off" and "on" STN or GPi stimulation in Parkinson's disease. Neurology. 2000; 55:411–418. [PubMed: 10932277]

Price CJ, Friston KJ. Cognitive conjunction: a new approach to brain activation experiments. NeuroImage. 1997; 5:261–270. [PubMed: 9345555]

Schmahmann, JD.; Doyon, J.; Toga, AW.; Petrides, M.; Evans, AC. MRI Atlas of the Human Cerebellum. Academic Press; San Diego: 2000.

Sestini S, Scotto di Luzio A, Ammannati F, et al. Changes in regional cerebral blood flow caused by deep-brain stimulation of the subthalamic nucleus in Parkinson's disease. J Nucl Med. 2002; 43:725–732. [PubMed: 12050315]

Strafella AP, Dagher A, Sadikot AF. Cerebral blood flow changes induced by subthalamic stimulation in Parkinson's disease. Neurology. 2003; 60:1039–1042. [PubMed: 12654980]

Su PC, Ma Y, Fukuda M, et al. Metabolic changes following subthalamotomy for advanced Parkinson's disease. Ann Neurol. 2001; 50:514–520. [PubMed: 11601502]

Su PC, Tseng HM, Liu HM, Yen RF, Liou HH. Subthalamotomy for advanced Parkinson disease. J Neurosurg. 2002; 97:598–606. [PubMed: 12296644]

Trošt M, Su PC, Barnes A, et al. Evolving metabolic changes during the first postoperative year after subthalamotomy. J Neurosurg. 2003; 99:872–878. [PubMed: 14609167]

Trošt M, Simon ES, Dhawan V, Okulski J, Fodstad H, Eidelberg D. Clinical and metabolic brain changes in tremor predominant Parkinson's disease patients treated with Vim DBS. Mov Disord. 2004; 19(S383)

Vafaee MS, Ostergaard K, Sunde N, Gjedde A, Dupont E, Cumming P. Focal changes of oxygen consumption in cerebral cortex of patients with Parkinson's disease during subthalamic stimulation. NeuroImage. 2004; 22:966–974. [PubMed: 15193628]

Vitek JL, Giroux M. Physiology of hypokinetic and hyperkinetic movement disorders: model for dyskinesia. Ann Neurol. 2000; 47:S131–S140. [PubMed: 10762140]

Wichmann T, DeLong MR. Functional and pathophysiological models of the basal ganglia. Curr Opin Neurobiol. 1996; 6:751–758. [PubMed: 9000030]

Windels F, Bruet N, Poupard A, et al. Effects of high frequency stimulation of subthalamic nucleus on extracellular glutamate and GABA in substantia nigra and globus pallidus in the normal rat. Eur J Neurosci. 2000; 12:4141–4146. [PubMed: 11069610]

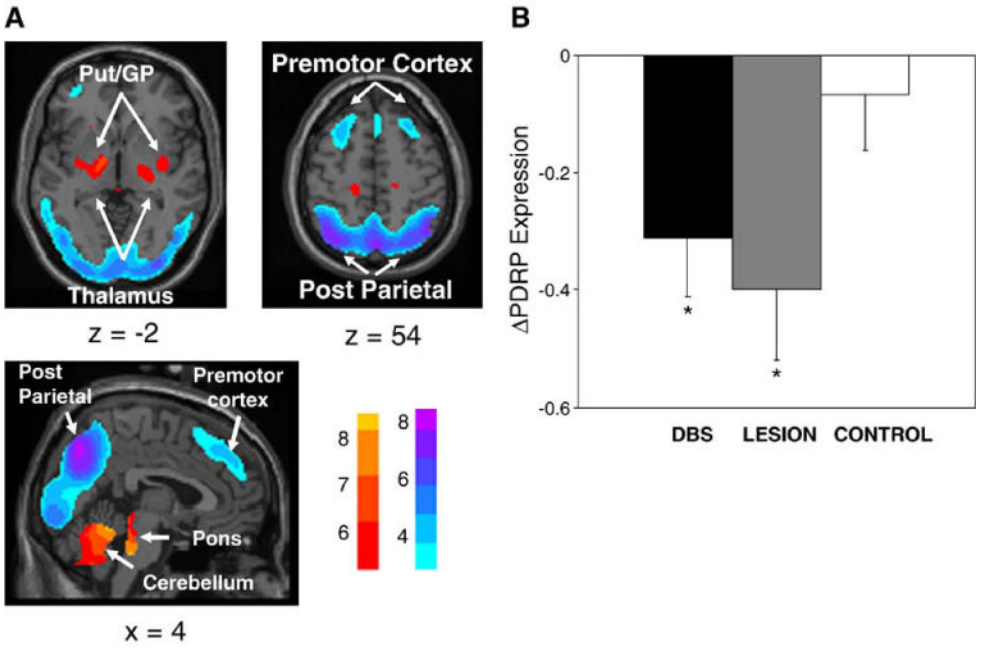

Fig. 1.

(A) Parkinson's disease-related pattern (PDRP) identified by network analysis of [^{18}F]-fluorodeoxyglucose (FDG) PET scans from 30 PD patients and 30 age-matched normal volunteer subjects. This pattern was characterized by relative metabolic increases in the pallidum and thalamus (left) and in the pons and cerebellum (bottom). These changes covaried with metabolic decreases in the lateral premotor and parieto-occipital association areas (right). [The display represents voxels that contribute significantly to the network at $P = 0.001$ and that were demonstrated to be reliable ($P < 0.001$) by bootstrap estimation (Efron and Tibshirani, 1994). Voxels with positive region weights (metabolic increases) are color coded from red to yellow; those with negative region weights (metabolic decreases) are color coded from blue to purple.] (B) Bar histogram of the change in PDRP expression (ΔPDRP; mean±SE) quantified in hemispheres undergoing either STN deep brain stimulation (DBS, filled bar) or lesioning (LESION, shaded bar), and in non-operated control hemispheres (CNTL, open bar). Significant reductions in network activity were observed with both interventions ($P < 0.05$, see text). However, the degree of network modulation was not different for the two treatment groups ($P = 0.58$). [Asterisks refer to comparisons with control hemispheres; $P < 0.05$].

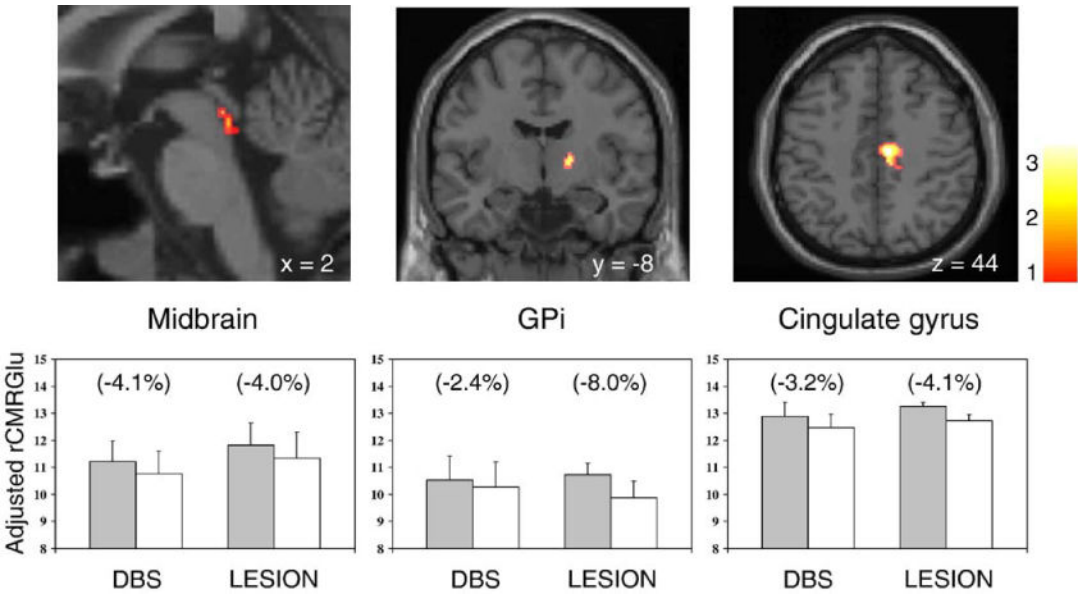

Fig. 2.

Top: regions with metabolic reductions occurring in both the STN stimulation and lesioning groups (Table 3; see text). Metabolic decrements with treatment were detected in the midbrain (left), the internal segment of the globus pallidus (GPi) (middle), and in the anterior cingulate region (right). [SPM{t}maps were superimposed on a single-subject MRI brain template; surgically treated hemispheres appear on the right.] Bottom: bar histograms illustrate rates of glucose utilization for each of the significant clusters displayed above. Metabolic values (mean±SE) are presented for each treatment condition. The treatment-induced decrease in GPi metabolism was greater in magnitude in the STN lesion group ($P < 0.01$). [OFF/PRE (filled bars) and ON/POST (open bars) correspond to the stimulation (DBS) and lesioning (LESION) groups, respectively. Regional changes with intervention appear in parenthesis.]

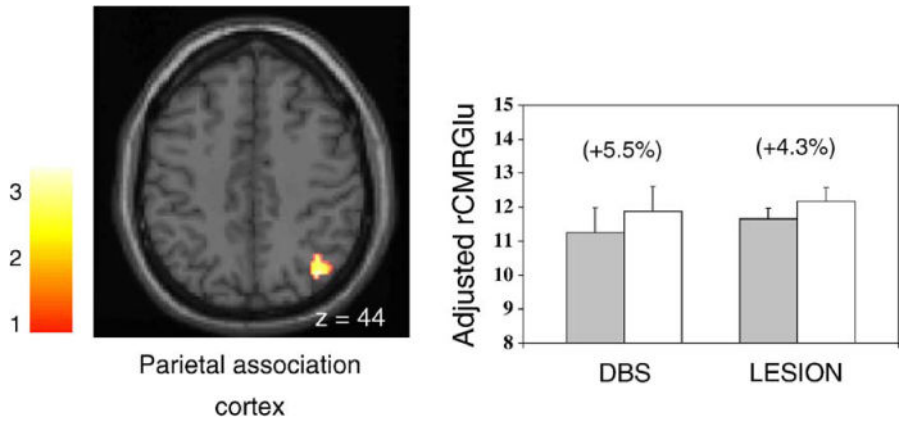

Fig. 3.

Left: regions with metabolic increases occurring in both STN stimulation and lesioning groups (see Table 3 and Fig. 2). Metabolic increases with treatment were detected in the parietal association cortex. [SPM{t}maps were superimposed on a single-subject MRI brain template; surgically treated hemisphere appears on the right.] Right: bar histograms illustrate rates of glucose utilization for the significant cluster in the posterior parietal cortex. Metabolic values (mean±SE) are presented for each treatment condition. The treatment-induced increase in parietal metabolism was greater in magnitude in the DBS group ($P < 0.05$). [OFF/PRE (filled bars) and ON/POST (open bars) correspond to the stimulation (DBS) and lesioning (LESION) groups, respectively. Regional changes with intervention appear in parenthesis.]

Table 1

Patient characteristics and stimulation parameters

Patient	Age (years)	Sex	Duration (years)	Stimulated side	Baseline UPDRS[a]	Stimulation parameters[b]		
						Pulse width (μs)	Frequency (Hz)	Amplitude (V)
1	59	M	7	R	48	60	130	2.3
2	69	M	14	L	60	60	130	2.8
3	61	F	12	R	50	60	130	2.0
4	47	M	12	R	72	90	160	2.6
5	58	M	7	B	40	60/60	160/145	2.8/1.7
6	66	M	10	B	43	60/60	145/130	2.8/2.6
Mean	60	5M/1F	10.3	4 Uni/2 Bil	52.2	63.8	141.3	2.5

[a] Composite Unified Parkinson's Disease Rating Scale (UPDRS) motor ratings obtained 12 h following the cessation of antiparkinsonian medication.

[b] Stimulation parameters for bilateral subjects are presented as Left/Right.

Table 2

Brain regions with significant metabolic changes following STN DBS

Brain region	Coordinates[a]			Z_{max}
	x	*y*	*z*	
Metabolic decreases				
Cerebellum, lobule VIIIA[b,*]	2	−66	−36	2.18
Midbrain[**]	0	−28	−10	3.08
Pons[*]	0	−30	−22	2.28
Precentral gyrus, BA 4[**]	40	−14	42	2.39
Supplementary motor area, BA 6[**]	6	−16	50	2.54
Metabolic increases				
Medial frontal gyrus, BA 9[*]	2	48	22	1.74
Parietal association cortex, BA 7[**]	38	−72	48	2.50

BA = Brodmann area.

[a] Montreal Neurological Institute (MNI) standard space.

[b] According to the atlas of Schmahmann et al. (2000).

[*] $P < 0.05$ (uncorrected, within hypothesis-testing mask).

[**] $P < 0.01$ (uncorrected, within hypothesis-testing mask).

Table 3

Brain regions with significant metabolic changes following both surgical interventions

Brain region	Coordinates[a]			Z_{max}
	x	*y*	*z*	
Metabolic decreases				
Midbrain*	2	−30	−12	2.56
GPi*	18	−8	4	2.67
Cingulate gyrus, BA 24/6*	8	−16	44	3.41
Metabolic increases				
Parietal cortex, BA 7/39/40*	38	−70	44	3.07

BA = Brodmann area; GPi = Internal globus pallidus.

[a]Montreal Neurological Institute (MNI) standard space.

*$P < 0.01$ (uncorrected, within hypothesis-testing mask).